

result in the desired $\lambda/4$ de Broglie wave effect³¹. In principle, this can be extended to higher-order interference effects because, obviously, when more than two double-pairs are emitted from the crystal the suppression of all lower-order interferences can be achieved by a proper projection analogous to the $N = 4$ case.

The method that we use here allows the generation of four-photon states and their subsequent utilization in pure four-particle interferometry. The result clearly confirms the theoretical expectation that the de Broglie wavelength of a four-photon state is one-quarter that of a single photon, thus leading to the general rule $\lambda(N) = \lambda(1)/N$. This overcomes the resolution limit of state-of-the-art two-particle interferometry, and opens new possibilities for multi-particle interference in fundamental quantum experiments and in applications such as quantum metrology. It is important to note that, in principle, this scheme can be extended to higher particle numbers if more spatial modes are involved. The actual limitation due to low count rates may eventually be overcome with the next generation of entangled photon sources and detectors. □

Received 14 November 2003; accepted 6 April 2004; doi:10.1038/nature02552.

1. Marton, L., Simpson, J. A. & Suddeth, J. A. Electron beam interferometer. *Phys. Rev.* **90**, 490–491 (1953).
2. Rauch, H., Treimer, W. & Bonse, U. Test of a single crystal neutron interferometer. *Phys. Lett. A* **47**, 369–371 (1974).
3. Keith, D. W., Ekstrom, C. R. & Pritchard, D. E. An interferometer for atoms. *Phys. Rev. Lett.* **66**, 2693–2696 (1991).
4. Arndt, M. *et al.* Wave-particle duality of C_{60} molecules. *Nature* **401**, 680–682 (1999).
5. Schrödinger, E. Die gegenwärtige Situation in der Quantenmechanik. *Naturwissenschaften* **23**, 807–812, 823–828, 844–849 (1935).
6. Horne, M. A. & Zeilinger, A. in *Symposium on the Foundations of Modern Physics* (eds Joensuu, L. P. & Mittelsted, P.) 435–439 (World Scientific Press, Singapore, 1985).
7. Greenberger, D., Horne, M. & Zeilinger, A. Multiparticle interferometry and the superposition principle. *Phys. Today* **8**, 22–29 (1993).
8. Lee, H., Kok, P. & Dowling, J. P. in *Proc. Sixth Int. Conf. on Quantum Communication, Measurement and Computing* (eds Shapiro, J. H. & Hirota, O.) 223–229 (Rinton Press, Princeton, 2002).
9. Yurke, B. Input states for enhancement of fermion interferometer sensitivity. *Phys. Rev. Lett.* **56**, 1515–1517 (1986).
10. Ou, Z. Y. Fundamental quantum limit in precision phase measurement. *Phys. Rev. A* **55**, 2598–2609 (1997).
11. Holland, M. J. & Burnett, K. Interferometric detection of optical phase shifts at the Heisenberg limit. *Phys. Rev. Lett.* **71**, 1355–1358 (1993).
12. Bollinger, J. J., Itano, W. M., Wineland, D. J. & Heinzen, D. J. Optimal frequency measurements with maximally correlated states. *Phys. Rev. A* **54**, R4649–R4652 (1996).
13. Boto, A. *et al.* Quantum interferometric optical lithography: Exploiting entanglement to beat the diffraction limit. *Phys. Rev. Lett.* **85**, 2733–2736 (2000).
14. de Steuarnagel, O. Broglie wavelength reduction for a multiphoton wave packet. *Phys. Rev. A* **65**, 033820 (2002).
15. Ou, Z. Y., Wang, L. J., Zou, X. Y. & Mandel, L. Evidence for phase memory in two-photon down conversion through entanglement with the vacuum. *Phys. Rev. A* **41**, 566–568 (1990).
16. Rarity, J. G. Two-photon interference in a Mach-Zehnder interferometer. *Phys. Rev. Lett.* **65**, 1348–1351 (1990).
17. Ou, Z. Y., Zou, X. Y., Wang, L. J. & Mandel, L. Experiment on nonclassical fourth-order interference. *Phys. Rev. A* **42**, 2957–2965 (1990).
18. Edamatsu, K., Shimizu, R. & Itoh, T. Measurement of the photonic de Broglie wavelength of entangled photon pairs generated by spontaneous parametric down-conversion. *Phys. Rev. Lett.* **89**, 213601 (2002).
19. Jacobson, J., Björk, G., Chuang, I. & Yamamoto, Y. Photonic de Broglie waves. *Phys. Rev. Lett.* **74**, 4835–4838 (2002).
20. Fonseca, E. J. S., Monken, C. H. & Padua, S. Measurement of the de Broglie wavelength of a multiphoton wave packet. *Phys. Rev. Lett.* **82**, 2868–2871 (1999).
21. Gerry, C. C. & Campos, R. A. Generation of maximally entangled photonic states with a quantum-optical Fredkin gate. *Phys. Rev. A* **64**, 063814 (2001).
22. Kok, P., Lee, H. & Dowling, J. Creation of large-photon number path entanglement conditioned on photodetection. *Phys. Rev. A* **65**, 052104 (2002).
23. Kwiat, P. G. *et al.* New high-intensity source of polarization-entangled photon pairs. *Phys. Rev. Lett.* **75**, 4337–4341 (1995).
24. Pan, J.-W., Gasparoni, S., Ursin, R., Weihs, G. & Zeilinger, A. Experimental entanglement purification of arbitrary unknown states. *Nature* **423**, 417–422 (2003).
25. Ou, Z. Y. & Mandel, L. Violation of Bell's inequality and classical probability in a two-photon correlation experiment. *Phys. Rev. Lett.* **61**, 50–53 (1988).
26. Shih, Y. H. & Alley, C. O. New type of Einstein-Podolsky-Rosen-Bohm experiment using pairs of light quanta produced by optical parametric down conversion. *Phys. Rev. Lett.* **61**, 2921–2924 (1988).
27. Weinfurter, H. & Zukowski, M. Four-photon entanglement from down-conversion. *Phys. Rev. A* **64**, 010102 (2001).
28. Simon, C. & Pan, J.-W. Polarization entanglement purification using spatial entanglement. *Phys. Rev. Lett.* **89**, 257901 (2002).
29. Hong, C. K., Ou, Z. Y. & Mandel, L. Measurement of subpicosecond time intervals between two photons by interference. *Phys. Rev. Lett.* **59**, 2044–2046 (1987).
30. Kok, P. *et al.* Quantum interferometric optical lithography: Towards arbitrary two-dimensional patterns. *Phys. Rev. A* **63**, 063407 (2001).

31. Lamas-Linares, A., Howell, J. C. & Bouwmeester, D. Stimulated emission of polarization-entangled photons. *Nature* **412**, 887–890 (2001).

Acknowledgements We thank Č. Brukner and K. Resch for discussions, and V. Scarani for comments on the manuscript. This work was supported by the Austrian Science Foundation (FWF), the European Commission in the RAMBOQ project and by the Alexander von Humboldt Foundation.

Competing interests statement The authors declare that they have no competing financial interests.

Correspondence and requests for materials should be addressed to A.Z. (zeilinger-office@quantum.at).

Super-resolving phase measurements with a multiphoton entangled state

M. W. Mitchell, J. S. Lundeen & A. M. Steinberg

Department of Physics, University of Toronto, 60 St George Street, Toronto, Ontario M5S 1A7, Canada

Interference phenomena are ubiquitous in physics, often forming the basis of demanding measurements. Examples include Ramsey interferometry in atomic spectroscopy, X-ray diffraction in crystallography and optical interferometry in gravitational-wave studies^{1,2}. It has been known for some time that the quantum property of entanglement can be exploited to perform super-sensitive measurements, for example in optical interferometry or atomic spectroscopy^{3–7}. The idea has been demonstrated for an entangled state of two photons⁸, but for larger numbers of particles it is difficult to create the necessary multiparticle entangled states^{9–11}. Here we demonstrate experimentally a technique for producing a maximally entangled three-photon state from initially non-entangled photons. The method can in principle be applied to generate states of arbitrary photon number, giving arbitrarily large improvement in measurement resolution^{12–15}. The method of state construction requires non-unitary operations, which we perform using post-selected linear-optics techniques similar to those used for linear-optics quantum computing^{16–20}.

Our goal is to create the state

$$|N :: 0\rangle_{a,b} \equiv \frac{1}{\sqrt{2}} (|N, 0\rangle_{a,b} + |0, N\rangle_{a,b}) \quad (1)$$

which describes two modes a, b in a superposition of distinct Fock states $|n_a = N, n_b = 0\rangle$ and $|n_a = 0, n_b = N\rangle$. This state figures in several metrology proposals, including atomic frequency measurements⁴, interferometry^{3,6,7}, and matter-wave gyroscopes⁵. In these proposals the particles occupying the modes are atoms or photons.

The advantage for spectroscopy can be seen in this idealization: we wish to measure a level splitting $H_{\text{ext}} = \epsilon_{ba} b^\dagger b$ between modes b and a using a fixed number of particles N in a fixed time T . We could prepare N copies of the single-particle state $(|1, 0\rangle_{a,b} + |0, 1\rangle_{a,b})/\sqrt{2}$ and allow them to evolve to the state $|\phi\rangle \equiv (|1, 0\rangle_{a,b} + \exp[i\phi]|0, 1\rangle_{a,b})/\sqrt{2}$, where $\phi = \epsilon_{ba} T/\hbar$. Measurements of $A_1 \equiv |0, 1\rangle\langle 1, 0| + |1, 0\rangle\langle 0, 1|$ on this ensemble give $\langle A_1 \rangle = \cos(\phi)$ with phase uncertainty at the shot-noise limit, $\Delta\phi = 1/\sqrt{N}$. In contrast, under the same hamiltonian $|N :: 0\rangle$ evolves to $(|N, 0\rangle + \exp[iN\phi]|0, N\rangle)/\sqrt{2}$. If we measure the operator $A_N \equiv$

$|0, N\rangle \langle N, 0| + |N, 0\rangle \langle 0, N|$, we find $\langle A_N \rangle = \cos(N\phi)$. The dependence on $N\phi$ rather than ϕ is phase super-resolution: one cycle of $\langle A_N \rangle$ implies a smaller change of ϕ (or ϵ_{ba}) than one cycle of $\langle A_1 \rangle$. Phase super-sensitivity, a reduction of phase uncertainty, is also predicted. A number of schemes have been proposed^{3-7,12,21,22} to reach the so-called Heisenberg limit $\Delta\phi = 1/N$. The simplest proposals would measure the operator A_N . This can be implemented with coincidence measurements, as the probability of detecting all N quanta in a mode $(a+b)/\sqrt{2}$ is proportional to $1 + \langle A_N \rangle$. Phase super-resolution has been demonstrated for $N=2$ with photons in a Mach-Zehnder interferometer^{23,24} and with trapped ions²⁵.

A related technique, quantum interferometric optical lithography, proposes using phase super-resolution to write features smaller than the single-photon diffraction limit. There the modes a, b are spatial, with different propagation directions. A molecule exposed to both modes and capable of absorbing N photons would, in effect, perform the measurement of A_N as above, with N -fold super-resolution in position. Using coincidence detection in place of two-photon absorbers, this principle has been demonstrated for $N=2$ using down-converted pairs⁸. In that experiment, as well as in the earlier Mach-Zehnder experiments, two infrared photons showed the same resolution or angular resolution as the blue pump photon that generated them, a factor of two improvement over the resolution of a single infrared photon. The question remains as to whether resolution can be improved beyond that of the photons used to generate the entangled state. Here we answer that question in the affirmative by constructing a multiparticle state with greater phase resolution than any of its single-particle precursors. The technique could in principle be used to generate entangled states of arbitrarily large N with arbitrarily good resolution.

We prepare the state $|3::0\rangle_{a,b}$ where the modes a and b are the horizontal (H) and vertical (V) polarizations of a single spatial mode. The construction of the polarization state is based on earlier proposals to construct photon-number path-entangled states¹²⁻¹⁴. A similar technique for polarization has recently been independently proposed¹⁵. The key to the construction is the fact that $|3::0\rangle_{a,b}$, when written in terms of creation operators a_a^\dagger and a_b^\dagger acting on the vacuum $|0\rangle$, is equal to

$$|3::0\rangle_{a,b} = (a_a^\dagger + a_b^\dagger)(a_a^\dagger + e^{i\chi}a_b^\dagger)(a_a^\dagger + e^{i2\chi}a_b^\dagger)|0\rangle \quad (2)$$

where $\chi = 2\pi/3$ and normalization has been omitted. The terms in parentheses each create a particle, but in non-orthogonal states. If a and b are left (L) and right (R) circular polarization, these states describe linear polarizations rotated by 60° from each other. Using post-selection, we can put one photon of each polarization into a single spatial mode and create $|3::0\rangle_{a,b}$.

We use two photons from pulsed parametric down-conversion plus one laser, or 'local oscillator' (LO), photon, adapting a technique first used to show non-classical interference of independent sources^{26,27}. Pulses of 100 fs duration and 810 nm centre wavelength are produced by a mode-locked Ti:sapphire laser and frequency-doubled, giving 405-nm pulses with an average power of 50 mW. These are gently focused into a 0.5-mm-thick β -barium borate crystal aligned for type-II parametric down-conversion in the 'collapsed cone' geometry²⁸. The down-converted (DC) photons thus produced are orthogonally polarized. A small part of the Ti:sapphire beam is split off and attenuated to contribute the LO photon. These three photons are transformed into the state $|3::0\rangle$ and detected by polarization-resolved threefold coincidence detection. The transformation (Fig. 1a) can be understood as a sequence of mode combinations. After the PBS, the DC photons are in the state $a_H^\dagger a_V^\dagger |0\rangle$, where subscripts indicate polarization. A half wave-plate rotates this to $a_{+45^\circ}^\dagger a_{-45^\circ}^\dagger |0\rangle$, where subscripts show linear polarizations measured from vertical. We perform the first post-selected non-unitary operation by passing the pair through three

plates of BK7 glass near the Brewster angle. The six Brewster-angle interfaces act as a partial polarizer (PP) with transmission efficiencies of $T_H \approx 1, T_V \approx 1/3$. By post-selecting cases where no photons are reflected, we transform the state as (again without normalization):

$$\begin{aligned} a_{+45^\circ}^\dagger a_{-45^\circ}^\dagger |0\rangle &= (a_H^\dagger + a_V^\dagger)(a_H^\dagger - a_V^\dagger)|0\rangle \\ &\rightarrow (a_H^\dagger + \frac{1}{\sqrt{3}}a_V^\dagger)(a_H^\dagger - \frac{1}{\sqrt{3}}a_V^\dagger)|0\rangle \quad (3) \\ &= a_{+60^\circ}^\dagger a_{-60^\circ}^\dagger |0\rangle \end{aligned}$$

This operation, putting orthogonally polarized photons into non-orthogonal modes, is non-unitary and requires post-selection.

The DC photons meet the LO photon at the last interface of the PP. This interface acts as a beamsplitter putting all three into the same spatial mode, conditioned on zero photons leaving by the 'dark' port. Again, the operation is non-unitary and requires post-selection. The LO photon is vertically polarized, and the state thus constructed is $a_0^\dagger a_{+60^\circ}^\dagger a_{-60^\circ}^\dagger |0\rangle$. This state has sixfold rotational symmetry about the beam propagation direction, and thus can only contain the states $|3, 0\rangle_{L,R}$ and $|0, 3\rangle_{L,R}$, where subscripts indicate the circular polarization basis¹⁵. In fact, it is easily verified that the state is $(|3, 0\rangle_{L,R} - |0, 3\rangle_{L,R})/\sqrt{2}$ up to an overall phase. Finally, we convert circular to linear polarizations with a quarter wave-plate, giving $(|3, 0\rangle_{H,V} - |0, 3\rangle_{H,V})/\sqrt{2}$. Ideally, the probability of both post-selections succeeding is $2 \cos^4(\pi/12)/3 \approx 58\%$.

Response to the phase shifter demonstrates phase super-resolution. Acting on a single photon, the quartz wedges shift by ϕ the phase of the V-polarization. Acting on three photons the phase shift is tripled: $|3::0\rangle_{H,V}$ becomes $|3::0\rangle_{H,V}^{3\phi} \equiv (|3, 0\rangle_{H,V} + \exp[i3\phi]|0, 3\rangle_{H,V})/\sqrt{2}$, where we have absorbed the negative sign above into the phase factor. The 3ϕ behaviour can be seen in threefold coincidence detection (triples detection) in the $\pm 45^\circ$

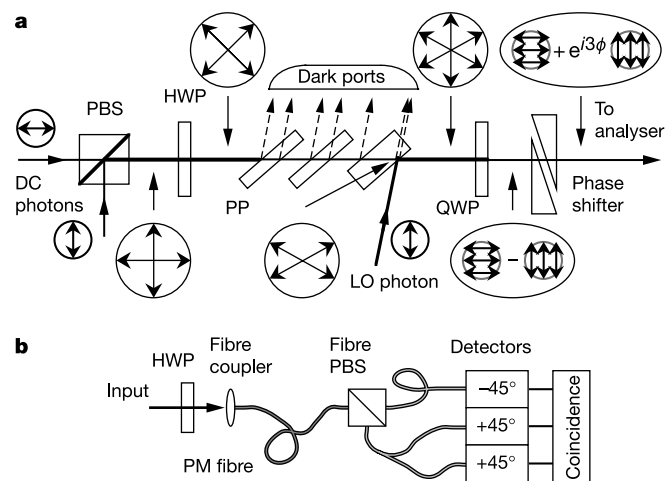


Figure 1 Diagram of production and detection of the state $|3::0\rangle_{H,V}^{3\phi}$. **a**, The chain of optical components and their effect on polarization state, represented in encircled figures. All photons have wavelength 810 nm. A polarizing beamsplitter (PBS) puts the DC photons in a single spatial mode and a half wave-plate (HWP) rotates their polarizations to $\pm 45^\circ$. A partial polarizer (PP) transforms the polarizations to $\pm 60^\circ$ if no photons are reflected into the dark ports. The LO photon is injected at the final interface of the partial polarizer. A quarter wave-plate (QWP) rotates to $(|3, 0\rangle_{H,V} - |0, 3\rangle_{H,V})/\sqrt{2}$ and quartz wedges produce an adjustable phase 3ϕ between the two components of the state. **b**, Analysis in the $\pm 45^\circ$ polarization basis is performed with a HWP before a polarization-maintaining (PM) fibre and a fibre-coupled PBS. The outputs of the fibre PBS are channelled to one, two or three detectors as needed. The configuration to detect $|2, 1\rangle_{\pm 45^\circ}$ is shown. Digital electronics record single detections as well as two- and three-fold coincidences.

linear polarization basis. The rates for detection of $|3, 0\rangle_{\pm 45^\circ}$ and $|2, 1\rangle_{\pm 45^\circ}$ vary as $1 \pm \cos(3\phi)$, respectively. After passing through an 810 nm wavelength filter with a 10 nm passband, the photons enter the polarization analyser, set to detect $|3, 0\rangle_{\pm 45^\circ}$ or $|2, 1\rangle_{\pm 45^\circ}$ (Fig. 1b).

The use of DC pairs removes the need for detectors at the ‘dark’ ports. Down-conversion very infrequently produces more than two photons in a single pulse, so we can infer with near-certainty the absence of photons in the ‘dark’ port from the presence of both photons in the ‘bright’ port. Using a weak coherent state to supply the third photon, we can make small the probability that more than one LO photon was present in a triple detection event⁴. Thus a single post-selection for threefold coincidence at the detectors performs at once the post-selections for both non-unitary operations.

Figure 2 shows results for detection of multiple polarizations at the analyser. Intensities of the DC and LO sources were adjusted such that one-photon detections (singles detections) are mostly produced by LO photons (about 10:1 ratio versus DC singles), twofold coincidences mostly by DC pairs (about 5:1 versus LO accidentals), and threefold coincidences principally by one LO photon plus one DC pair (about 2:1 versus accidental triples contributions, below). Thus with a single scan of the phase shifter we can see qualitatively different behaviours for states of one, two and three photons. Figure 2c clearly shows oscillation with 3ϕ , as predicted by theory. The resolution exceeds that achievable with any single photon in the experiment. The 405-nm photons would show oscillation with 2.1ϕ owing to their shorter wavelength and the somewhat larger birefringence of quartz at that wavelength. The observed 3ϕ oscillation is analogous to multipath interference:

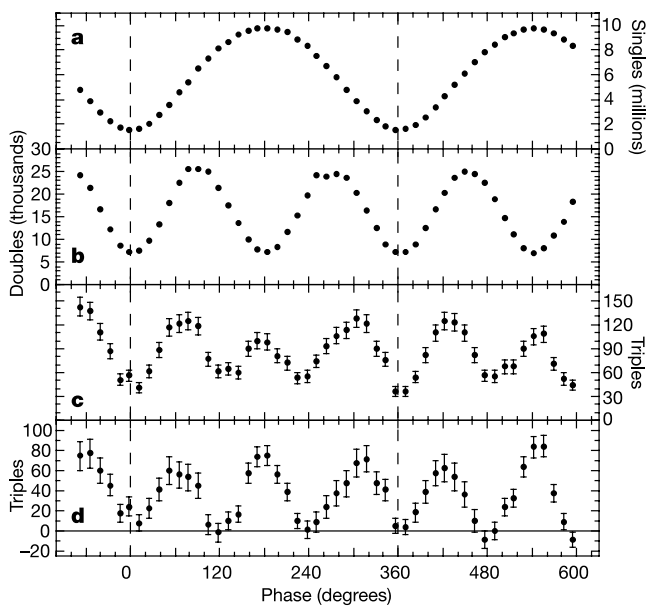


Figure 2 Super-resolving phase measurement with two and three photons. The polarization analyser is configured with one detector on the -45° output and two on $+45^\circ$. The input, a combination of down-converted and laser photons, is constructed to give the state $|3 :: 0\rangle_{H,V}^{3\phi}$ upon post-selection (see text). All graphs show detections per 30-s counting interval as the phase ϕ is changed by translating a phase-shifter prism. **a**, Singles detection at -45° , that is, detection of $|0, 1\rangle_{\pm 45^\circ}$, shows oscillation with ϕ . **b**, Two-fold coincidence detection of $|1, 1\rangle_{\pm 45^\circ}$ shows oscillation with 2ϕ . **c**, Three-fold coincidence detection of $|2, 1\rangle_{\pm 45^\circ}$ shows oscillation with 3ϕ . Error bars indicate $\pm\sigma$ statistical uncertainty. **d**, Three-fold coincidence after background subtraction. Error bars show $\pm\sigma$ statistical uncertainty plus a systematic uncertainty in the background. Dashed vertical bars indicate one full cycle.

Because the DC and LO photons are indistinguishable, there are several different ‘paths’ to the single outcome $|2, 1\rangle_{\pm 45^\circ}$. For example, the LO photon could go to the -45° detector and the two DC photons to $+45^\circ$. This path interferes with other permutations to give the signal shown in Fig. 2c. A cosine curve fitted to these data shows a visibility of $42 \pm 3\%$. This visibility is unambiguous evidence of indistinguishability and entanglement among the three photons. A non-entangled state of three distinguishable photons could also show threefold coincidence oscillation at 3ϕ , but with a maximal visibility of 20%.

Figure 2d shows the same triples data after subtraction of background from accidental triples. In addition to the signal of interest from 1 DC pair + 1 LO photon, we also see events from 2 DC pairs, from 3 LO photons, and from 2 LO photons + 1 DC pair. We calculate these backgrounds from independent measurements of single and double detection rates for the DC and LO sources alone. Coincidence background is calculated by the statistics of uncorrelated sources using a time-window of 12.5 ns, the laser pulse period. Incoherence of the various contributions is ensured by sweeping the path length of the LO photon over $\pm 2 \mu\text{m}$ during acquisition. The calculated background has some variation with ϕ , so it is important to note that it is qualitatively different from the observed 3ϕ signal. Per 30-s interval, the accidental background contributes 22 ± 1 as a constant component, an average of 23 ± 1 oscillating with 2ϕ , 4 ± 1 with 1ϕ and <1 with 3ϕ . Here and elsewhere, uncertainty in the counting circuitry’s dead-time introduces a systematic error.

It is also possible to see 3ϕ behaviour detecting a single polarization (Fig. 3). This measurement corresponds to the original proposals for atomic spectroscopy and lithography^{4,12}. It gives a far weaker signal, in part because the maximum overlap of the state $|3 :: 0\rangle_{H,V}^{3\phi}$ with $|3, 0\rangle_{\pm 45^\circ}$ is smaller than with $|2, 1\rangle_{\pm 45^\circ}$. Also, the chance that all three photons go to distinct detectors (as needed for coincidence detection) is smaller for $|3, 0\rangle_{\pm 45^\circ}$. With these limitations, we are able to see the 3ϕ behaviour, but only by subtracting a considerable coincidence background.

Using linear optical elements and post-selection, we have constructed a multiparticle entangled state useful for super-resolving phase measurements. The demonstrated resolution is not only better than for a single infrared photon, it is better than could be achieved with any single photon in the experiment, including the down-conversion pump photons. Given the difficulty of generating coherent short-wavelength sources, this is encouraging for the

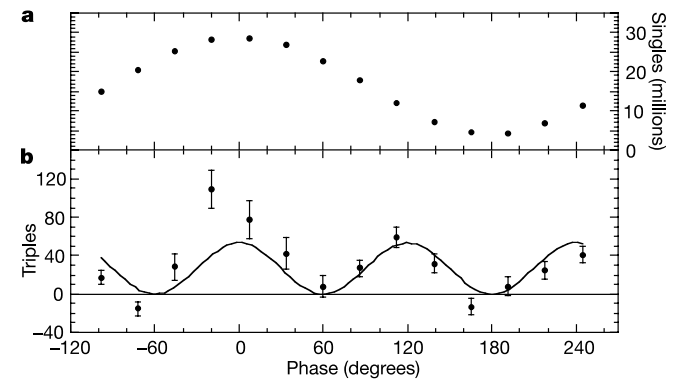


Figure 3 Super-resolving phase measurement with a single detected polarization. The polarization analyser is configured to detect $|3, 0\rangle_{\pm 45^\circ}$, that is, with three detectors on the $+45^\circ$ channel. The input state is the same as in Fig. 2. Graphs show detections per 300-s counting interval as the phase ϕ is changed. **a**, Singles detection shows oscillation with ϕ . **b**, Three-fold coincidence detection (after background subtraction) shows oscillation with 3ϕ . Error bars show $\pm\sigma$ statistical uncertainty plus a systematic uncertainty in the background. Curve is the expected signal $A[1 + \cos(3\phi)]$ with A chosen for best fit.

prospects of proposals such as quantum-interferometric optical lithography. The method can be adapted to generate entangled states of arbitrarily large photon number. Because prior entanglement is not required, the procedure would work well with single-photon-on-demand sources^{29,30}, which promise to be more efficient and scalable than down-conversion sources. Scalability would also be enhanced by the use of photon-number-resolving detectors. The construction proceeds from spatially separated, unentangled photons to a maximally entangled state in a single spatial mode, a state suitable for Heisenberg-limited phase measurements. □

Received 22 December 2003; accepted 16 March 2004; doi:10.1038/nature02493.

1. Barish, B. C. & Weiss, R. LIGO and the detection of gravitational waves. *Phys. Today* **52**, 44–50 (1999).
2. Caron, B. *et al.* The Virgo interferometer. *Class. Quantum Gravity* **14**, 1461–1469 (1997).
3. Holland, M. J. & Burnett, K. Interferometric detection of optical-phase shifts at the Heisenberg limit. *Phys. Rev. Lett.* **71**, 1355–1358 (1993).
4. Bollinger, J. J., Itano, W. M., Wineland, D. J. & Heinzen, D. J. Optimal frequency measurements with maximally correlated states. *Phys. Rev. A* **54**, R4649–R4652 (1996).
5. Dowling, J. P. Correlated input–port, matter-wave interferometer: Quantum-noise limits to the atom-laser gyroscope. *Phys. Rev. A* **57**, 4736–4746 (1998).
6. Ou, Z. Y. Fundamental quantum limit in precision phase measurement. *Phys. Rev. A* **55**, 2598–2609 (1997).
7. Campos, R. A., Gerry, C. C. & Benmoussa, A. Optical interferometry at the Heisenberg limit with twin Fock states and parity measurements. *Phys. Rev. A* **68**, 023810 (2003).
8. D’Angelo, M., Chekhova, M. V. & Shih, Y. Two-photon diffraction and quantum lithography. *Phys. Rev. Lett.* **87**, 013602 (2001).
9. Sackett, C. A. *et al.* Experimental entanglement of four particles. *Nature* **404**, 256–259 (2000).
10. Rauschenbeutel, A. *et al.* Step-by-step engineered multiparticle entanglement. *Science* **288**, 2024–2028 (2000).
11. Zhao, Z. *et al.* Experimental violation of local realism by four-photon Greenberger–Horne–Zeilinger entanglement. *Phys. Rev. Lett.* **91**, 180401 (2003).
12. Kok, P., Lee, H. & Dowling, J. P. Creation of large-photon-number path entanglement conditioned on photodetection. *Phys. Rev. A* **65**, 052104 (2002).
13. Fiurasek, J. Conditional generation of n-photon entangled states of light. *Phys. Rev. A* **65**, 053818 (2002).
14. Pryde, G. J. & White, A. G. Creation of maximally entangled photon-number states using optical fiber multiports. *Phys. Rev. A* **68**, 052315 (2003).
15. Hofmann, H. F. Generation of highly non-classical n-photon polarization states by super-bunching at a photon bottleneck. Preprint at (<http://arxiv.org/quant-ph/0311198>) (2003).
16. Knill, E., Laflamme, R. & Milburn, G. J. A scheme for efficient quantum computation with linear optics. *Nature* **409**, 46–52 (2001).
17. Franson, J. D., Donegan, M. M., Fitch, M. J., Jacobs, B. C. & Pittman, T. B. High-fidelity quantum logic operations using linear optical elements. *Phys. Rev. Lett.* **89**, 137901 (2002).
18. Resch, K. J., Lundeen, J. S. & Steinberg, A. M. Conditional-phase switch at the single-photon level. *Phys. Rev. Lett.* **89**, 037904 (2002).
19. Mitchell, M. W., Ellenor, C. W., Schneider, S. & Steinberg, A. M. Diagnosis, prescription, and prognosis of a Bell-state filter by quantum process tomography. *Phys. Rev. Lett.* **91**, 120402 (2003).
20. O’Brien, J. L., Pryde, C. J., White, A. G., Ralph, T. C. & Branning, D. Demonstration of an all-optical quantum controlled-NOT gate. *Nature* **426**, 264–267 (2003).
21. Sanders, B. C., Milburn, G. J. & Zhang, Z. Optimal quantum measurements for phase-shift estimation in optical interferometry. *J. Mod. Opt.* **44**, 1309–1320 (1997).
22. Huelga, S. F. *et al.* Improvement of frequency standards with quantum entanglement. *Phys. Rev. Lett.* **79**, 3865–3868 (1997).
23. Rarity, J. G. *et al.* 2-photon interference in a Mach-Zehnder interferometer. *Phys. Rev. Lett.* **65**, 1348–1351 (1990).
24. Ou, Z. Y., Zou, X. Y., Wang, L. J. & Mandel, L. Experiment on nonclassical 4th-order interference. *Phys. Rev. A* **42**, 2957–2965 (1990).
25. Meyer, V. *et al.* Experimental demonstration of entanglement-enhanced rotation angle estimation using trapped ions. *Phys. Rev. Lett.* **86**, 5870–5873 (2001).
26. Rarity, J. C. & Tapster, P. R. Three-particle entanglement from entangled photon pairs and a weak coherent state. *Phys. Rev. A* **59**, R35–R38 (1999).
27. Rarity, J. G., Tapster, P. R. & Loudon, R. Nonclassical interference between independent sources. Preprint at (<http://arxiv.org/quant-ph/9702032>) (1997).
28. Takeuchi, S. Beamlike twin-photon generation by use of type II parametric down-conversion. *Opt. Lett.* **26**, 843–845 (2001).
29. Michler, P. *et al.* A quantum dot single-photon turnstile device. *Science* **290**, 2282–2285 (2000).
30. Solomon, G. S., Pelton, M. & Yamamoto, Y. Single-mode spontaneous emission from a single quantum dot in a three-dimensional microcavity. *Phys. Rev. Lett.* **86**, 3903–3906 (2001).

Acknowledgements We thank K. Resch and J. O’Brien for discussions, and J. Dowling and D. R. Schumliar for inspiration. This work was supported by the National Science and Engineering Research Council of Canada, Photonics Research Ontario, the Canadian Institute for Photonic Innovations and the DARPA-QuIST program.

Competing interests statement The authors declare that they have no competing financial interests.

Correspondence and requests for materials should be addressed to M.W.M. (mitchell@physics.utoronto.ca).

Increased seasonality in Middle East temperatures during the last interglacial period

Thomas Felis^{1,2}, Gerrit Lohmann^{1,2}, Henning Kuhnert², Stephan J. Lorenz³, Denis Scholz⁴, Jürgen Pätzold^{1,2}, Saber A. Al-Rousan⁵ & Salim M. Al-Moghrabi^{5*}

¹DFG Forschungszentrum Ozeanränder, ²Fachbereich Geowissenschaften, Universität Bremen, 28359 Bremen, Germany

³Max-Planck-Institut für Meteorologie, Modelle & Daten, 20146 Hamburg, Germany

⁴Heidelberger Akademie der Wissenschaften, 69120 Heidelberg, Germany

⁵Marine Science Station, University of Jordan & Yarmouk University, 77110 Aqaba, Jordan

* Present address: Aqaba Special Economic Zone Authority, 77110 Aqaba, Jordan

The last interglacial period (about 125,000 years ago) is thought to have been at least as warm as the present climate¹. Owing to changes in the Earth’s orbit around the Sun, it is thought that insolation in the Northern Hemisphere varied more strongly than today on seasonal timescales², which would have led to corresponding changes in the seasonal temperature cycle³. Here we present seasonally resolved proxy records using corals from the northernmost Red Sea, which record climate during the last interglacial period, the late Holocene epoch and the present. We find an increased seasonality in the temperature recorded in the last interglacial coral. Today, climate in the northern Red Sea is sensitive to the North Atlantic Oscillation^{4,5}, a climate oscillation that strongly influences winter temperatures and precipitation in the North Atlantic region. From our coral records and simulations with a coupled atmosphere–ocean circulation model, we conclude that a tendency towards the high-index state of the North Atlantic Oscillation during the last interglacial period, which is consistent with European proxy records^{6–8}, contributed to the larger amplitude of the seasonal cycle in the Middle East.

The Arctic Oscillation/North Atlantic Oscillation (AO/NAO), the Northern Hemisphere’s dominant mode of atmospheric variability, exerts a strong influence on mid- and high-latitude continental climate by modulating the strength of the subpolar westerlies at interannual to interdecadal timescales^{9,10}. Previous work has shown that the northernmost Red Sea represents a location to study past AO/NAO-related atmospheric variability over the Northern Hemisphere, and that annually banded corals from this subtropical site provide proxy records of this variability over the past centuries^{4,5}. This narrow, desert-enclosed ocean basin is influenced by mid-latitude continental climate^{5,11} and is sensitive to atmospheric processes owing to a weak water column stratification¹².

Two fossil coral colonies (*Porites*) were collected near Aqaba on the Jordanian coast of the Gulf of Aqaba, the northeastern extension of the northernmost Red Sea (Fig. 1a). Colony AQB-10-B was recovered from a canal cut into the modern reef flat, whereas colony AQB-3-A was collected from a complex of raised reef terraces. X-radiographs revealed annual density bands and were used to identify areas within the colonies that appear to be unaffected by diagenetic alteration (Fig. 1b, c). X-ray diffraction analyses of these areas indicate an aragonite content of 98–99%, and petrographic thin sections show only traces of secondary aragonite. The bimonthly resolution time series of both coral $\delta^{18}\text{O}$ and $\delta^{13}\text{C}$ (not shown) generated from these areas show clear annual cycles, suggesting that the sampled sections were not subject to major diagenetic alterations with respect to stable isotopes (see Methods and Supplementary Information).